On Massive MIMO for Low Power Wide Area Networks

Felipe A. P. de Figueiredo*‡§, Claudio F. Dias‡§, Ingrid Moerman*, Eduardo R. de Lima†, and Gustavo Fraidenraich‡
*Ghent University–imec, IDLab, Department of Information Technology, Ghent, Belgium.
†Eldorado Research Institute, Campinas, Brazil.
‡DECOM/FEEC–State University of Campinas (UNICAMP), Campinas Brazil.
Email: *[felipe.pereira, ingrid.moerman]@ugent.be, †eduardo.lima@eldorado.org.br,
‡[aplnx, gf]@decom.fee.unicamp.br
§These authors contributed equally to this work.

***Abstract*—The use of large-scale antenna arrays grants considerable benefits in energy and spectral efficiency to wireless systems due to spatial resolution and array gain techniques. By assuming a dominant line-of-sight environment in a massive MIMO scenario with favorable propagation, we derive analytical expressions for the sum-capacity. Then, we show that convenient simplifications on the sum-capacity expressions are possible when working at low and high SNR regimes. Furthermore, in the case of a high SNR regime, it is demonstrated that the Gamma PDF can approximate the PDF of the instantaneous channel sum-capacity as the number of BS antennas grows. A second important demonstration presented in this work is that a Gamma PDF can also be used to approximate the PDF of the summation of the channel's singular values as the number of devices increases. Finally, it is important to highlight that the presented framework is useful for LPWAN's as we show that the transmit power of each device can be made inversely proportional to the number of BS antennas.**

***Index Terms*—massive MIMO, LPWAN, channel capacity, outage probability.**

I. Introduction

During the past years, we have been witnessing Massive MIMO becoming an efficient and indispensable sub-6 GHz physical-layer technology for wireless and mobile networks. The embodiment of such technology was vital for the current 5G New Radio (NR) interface [1]. The central concept behind Massive MIMO is the use of a large antenna array deployed at base stations (BS) to simultaneously serve a large number of devices over the same time-frequency resources. In this way, the technique allows exploiting differences among the propagation signatures of the devices in order to perform spatial multiplexing [1]. Even though the Massive MIMO technology looks quite mature, being adopted by new standards, it does not mean an end for research in this subject but just the beginning of unforeseen possibilities [2].

Current requirements for next-generation networks such as high bit rates, very low latency, high energy efficiency, and link robustness are not wholly met even by the current 5G solutions. Thus, there are still several open challenges that need to be addressed by researchers.

One of the approaches used to increase throughput is by increasing the network density, that is, decreasing the size and increasing the number of cells in the same coverage area. As a result, the size of the cells is becoming smaller and smaller, and consequently, it is quite probable that wireless channels will be predominantly line-of-sight (LOS) [3]. Furthermore, the LOS characteristic becomes even more apparent as technology moves to millimeter-wave bands in order to fulfill the requirements for wider bandwidths ($i.e.$, micro and femtocells) [4], [5].

Smart farming and rural broadband services provision ($i.e.$, distant areas with low population density) stewards a significant gap in the research body of Massive MIMO nowadays [6], [7]. In the sense of wireless services, it is essential to observe that most economically viable areas for agriculture are the plain terrains with few obstacles [8]. Thus, since the multipath-channel statistics of rural and distant areas are different from those found in urban centers, the wireless channel will likely to be predominantly LOS in such areas [9], [10].

Another critical research opportunity is the application of Massive MIMO to communications with unmanned aerial vehicles (UAVs) or also known as drones [11]. As with the other examples, these communications will probably be LOS-based as well.

Among the approaches and opportunities cited here, low power wide area networks (LPWANs) for drones, sensors, automated processes, etc. [12] pose several unsolved research challenges. For example, in the near future, swarms of drones, equipped with LPWAN devices, will be flying everywhere for applications ranging from surveillance to goods' delivery [13]–[15]. These devices will be always moving around the cell at different speeds and positions with a dominant LOS link to the BS. The sum-capacity achieved by a BS serving a massive number of drones, which have a dominant LOS link to the BS and are constantly moving around the cell is still an open issue.

Therefore, in this work, we assume a dominant LOS environment in a massive MIMO scenario with favorable propagation serving a massive number of devices constantly moving within the cell. With this aspect in mind, the objective of this investigation is to find capacity limits concerning the number of devices, number of base station antennas, and SNR. More specifically, the contributions of this work are as follows.

Preprints (www.preprints.org) | NOT PEER-REVIEWED | Posted: 3 November 2019 doi:10.20944/preprints201911.0021.v1

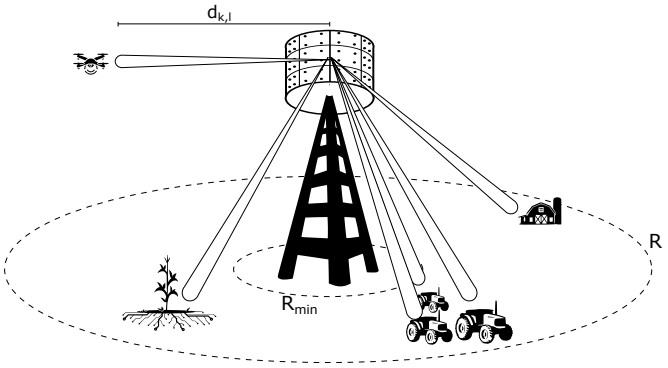

Figure 1. Illustration of the adopted system model.

- Derive an analytical expression for the channel sum-capacity.
- Show that the transmit power of each device can be made inversely proportional to the number of BS antennas.
- Find analytical expressions for the upper and lower-bound channel sum-capacities.
- Present expressions for the channel sum-capacity in low and high SNR regimes.
- Demonstrate that the Gamma PDF can approximate the PDF of the instantaneous channel sum-capacity in a high SNR regime as the number of antennas increase.
- Demonstrate that a Gamma PDF can also approximate the PDF of the summation of the channel's singular values as the number of devices increases.

The remaining of this paper is organized as follows: Section II presents the system model adopted in this work while Section III discusses aspects of favorable propagation in the current investigated conditions. Section IV review the concept of favorable propagation. Section V presents the results with parameters from reference systems. Finally, we close our discussion in the Section VI summarizing our conclusions.

II. System Model

Here we present the channel model adopted in [1]. We assume a channel model with only free-space non-fading ($i.e.$, pure) LOS propagation between the BS and the devices. Additionally, we also consider that the k-th device is located in the far-field of the antenna array. Therefore,

$$\mathbf{G} = \mathbf{H}\mathbf{Q}^{1/2} \tag{1}$$

where $h_{mk} = e^{-j\theta(m,k)}$, and the elements of the diagonal matrix $\mathbf{Q}$ are given as $q_{kk} = \beta_k$, and $\theta(m,k)$ models the devices' angular locations ($i.e.$ can be an arbitrary geometry configuration such as linear/rectangular uniform array) along with a random phase shift associated with a random range between the antenna array and the k-th device.

The free space path-loss coefficients, β_{km}, can be modeled as described in [16], there it is defined as

$$\beta_{km} = \frac{\eta}{d_{k,m}^2}, \tag{2}$$

where η is a constant equal to $\left(\frac{\lambda}{4\pi}\right)^2$ [17], $d_{k,m}$ is the distance between the m-th BS antenna and the k-th terminal's antenna, and the path-loss exponent is equal to 2, which is the value used for free-space propagation. As the distance between the k-th device and the antenna array is $d_{k,m} \gg \lambda$, then $d_{k,m} \approx d_k$, and consequently $\beta_{km} \approx \beta_k$, $i.e.$, β_{km} does not depend on the antenna index as the distance between the kth device and the BS is much greater than the distance between the antennas. We consider that d_k is an uniformly distributed random variable distributed in the interval $[R_{\text{min}}, R]$, where R_{min} is the minimum distance a device can be from the BS and R is the cell radius. The adopted system model is depicted in Figure 1.

III. Channel Sum-Capacity in LoS and Favorable Propagation Conditions

The distance between the device's antennas and the BS's antennas is not static as the devices are always moving within the cell ($e.g.$, drones, cars, etc.). Therefore, the distance has to be treated as a random variable, resulting in a different channel realization for every time instant. As it is known [1], the instantaneous sum-capacity is not a meaningful performance metric under such random conditions. Here, we are interested in the capacity performance averaged over all different positions a device might be within the cell. Therefore, in order to assess the performance in this scenario, we need to employ the notion of ergodic capacity, which results in the following uplink sum link capacity [18]

$$\begin{aligned} C &= \mathbb{E}\left[\log_2|\mathbf{I}_M + \rho\mathbf{G}\mathbf{G}^H|\right] \\ &= \mathbb{E}\left[\log_2|\mathbf{I}_K + \rho\mathbf{G}^H\mathbf{G}|\right]. \end{aligned} \tag{3}$$

where ρ is the average signal-to-interference ratio (SNR) and the expectation is taken over the joint distribution of all possible positions of the devices. As the additive white noise is assumed to have mean and variance equal to 0 and 1 respectively, therefore, ρ has, consequently, the interpretation of normalized *transmit* SNR and is therefore dimensionless [19]. It is important to highlight that the expectation in (3) is taken in relation with devices' channels, more specifically in relation with their positions within the cell ($i.e.$, distances and angles of arrival), which are considered as random variables. The second line of (3) is found by applying the Sylvester's determinant theorem. Furthermore, we assume that the base station has perfect knowledge of the channel matrix $\mathbf{G}$. Finding the exact ergodic capacity given by (3) is a quite complex task that involves finding the distribution of the eigenvalues of $\mathbf{G}^H\mathbf{G}$ [20]. In this work, as we will show next, we are concerned with finding the sum-capacity considering a Massive MIMO scenario and asymptotic favorable propagation [1]. Then, the sum-capacity in (3) can be re-expressed as

$$\begin{aligned} C &= \mathbb{E}\left[\log_2\left|\mathbf{I}_K + \rho\mathbf{G}^H\mathbf{G}\right|\right] \\ &\leq \mathbb{E}\left[\log_2\left(\prod_{k=1}^{K}\left[\mathbf{I}_K + \rho\mathbf{G}^H\mathbf{G}\right]_{k,k}\right)\right] \\ &= \mathbb{E}\left[\sum_{k=1}^{K}\log_2\left(\left[\mathbf{I}_K + \rho\mathbf{G}^H\mathbf{G}\right]_{k,k}\right)\right] \\ &= \mathbb{E}\left[\sum_{k=1}^{K}\log_2\left(1 + \rho\|\mathbf{g}_k\|^2\right)\right]. \end{aligned} \tag{4}$$

Preprints (www.preprints.org) | NOT PEER-REVIEWED | Posted: 3 November 2019 doi:10.20944/preprints201911.0021.v1

The inequality in the second line of (4) is found applying the Hadamard inequality and assuming that $\|\mathbf{g}_k\|^2, \forall k$ is known. As will be shown latter, this bound will be proven to be very tight. The equality in the second line of (4) holds if and only if $\mathbf{G}^H\mathbf{G}$ is a diagonal matrix ($i.e.$, the channel matrix $\mathbf{H}$ has mutually orthogonal columns) that must satisfy [21],

$$\mathbf{g}_i^H \mathbf{g}_j = \begin{cases} 0, & i,j = 1,\ldots,K, \text{ for } i \neq j \\ \|\mathbf{g}_k\|^2 = M\beta_k, & k = 1,\ldots,K, \text{ for } i = j, \end{cases} \tag{5}$$

which is the case when the channel exhibits favorable propagation [22]. The equality $\|\mathbf{g}_k\|^2 = M\beta_k$ is detailed in Appendix A. Given the assumption of channels exhibiting favorable propagation, the results presented in this work hold for any type of antenna array, $e.g.$, uniform linear array (ULA), uniform rectangular array (URA), etc.

Now using $\|\mathbf{g}_k\|^2 = M\beta_k$ and $\beta_k = \frac{\eta}{d_k^2}$ in the last line of (4), the sum-capacity upper bound can be re-written as

$$\begin{aligned} C &= \sum_{k=1}^{K} \mathbb{E}\left[\log_2\left(1 + \frac{\rho M \eta}{d_k^2}\right)\right] \\ &= K\mathbb{E}\left[\log_2\left(1 + \frac{\rho M \eta}{d_k^2}\right)\right], \end{aligned} \tag{6}$$

where the last equality is due to the fact that d_k is an i.i.d. random variable for all i.

Next, considering $z = \frac{1}{d_k^2}$ as a random variable denoted by Z with probability density function (PDF) given by

$$f_Z(z) = \frac{1}{2(R - R_{min})z\sqrt{z}}, \quad \frac{1}{R^2} \leq z \leq \frac{1}{R_{min}^2}, \tag{7}$$

then, (6) can be re-expressed as

$$\begin{aligned} C &= K\mathbb{E}\left[\log_2\left(1 + \frac{\rho M \eta}{d_k^2}\right)\right] \\ &= K\mathbb{E}\left[\log_2\left(1 + \rho M \eta z\right)\right] \\ &= \frac{K}{2(R - R_{min})}\int_{1/R^2}^{1/R_{min}^2} \log_2(1 + \rho M \eta z)\frac{1}{z\sqrt{z}}dz, \end{aligned} \tag{8}$$

where the proof of (7) is given in Appendix B. Next, solving (8) with an integral solver [23], we find an exact closed-form expression given in (9) for the capacity when the channel offers favorable propagation.

Remark 1: After analyzing (9), we see that if we make the transmit power of each device equal to P/M^α, where $\alpha > 1$, then the sum-capacity, C, will go to zero as $M \to \infty$. When $\alpha < 1$ the sum-capacity grows without bound as $M \to \infty$. This means that $1/M$ ($i.e.$, $\alpha = 1$) is the fastest rate at which we can decrease the transmit power of each device and still have a fixed capacity as $M \to \infty$.

Remark 1 clearly shows that as M grows without bound, the transmit power of each device can be reduced proportionally to $1/M$ and that the spectral efficiency increases by a factor of K, meaning that the BS can simultaneously serve K devices over the same time-frequency resources. This reduction of the transmit power per device is very important to power-constrained devices such as IoT devices.

A. A lower-bound for the Capacity

First we define the following Jensen's Inequality [24]

$$\mathbb{E}\left[\log_2(1+z)\right] \geq \log_2\left(1 + \frac{1}{\mathbb{E}\left[\frac{1}{z}\right]}\right), \tag{11}$$

where $z = \frac{1}{u}$ for $z > 0$. Therefore, (6) can be re-written as

$$\begin{aligned} C &= K\mathbb{E}\left[\log_2\left(1 + \frac{\rho M \eta}{d_k^2}\right)\right] \\ &\geq K\log_2\left(1 + \frac{\rho M \eta}{\mathbb{E}\left[d_k^2\right]}\right). \end{aligned} \tag{12}$$

Remembering that $f_d(r) = \frac{1}{R - R_{\min}}$, $R_{\min} \leq r \leq R$, then

$$\mathbb{E}\left[d_k^2\right] = \frac{R^3 - R_{min}^3}{3(R - R_{min})}. \tag{13}$$

For proof of (13), see Appendix D. Therefore, (12) can be re-expressed as

$$C \geq K\log_2\left(1 + \frac{3\rho M \eta (R - R_{min})}{R^3 - R_{min}^3}\right). \tag{14}$$

B. An upper-bound for the Capacity

Again, we can use the Jensen's Inequality as

$$\mathbb{E}\left[\log_2(1+z)\right] \leq \log_2\left(1 + \mathbb{E}\left[z\right]\right), \tag{15}$$

for $z > 0$. Therefore, (6) can be re-written as

$$\begin{aligned} C &= K\mathbb{E}\left[\log_2\left(1 + \frac{\rho M \eta}{d_k^2}\right)\right] \\ &\leq K\log_2\left(1 + \rho M \eta \mathbb{E}\left[\frac{1}{d_k^2}\right]\right). \end{aligned} \tag{16}$$

Remembering that $f_d(r) = \frac{1}{R - R_{\min}}$, $R_{\min} \leq r \leq R$, then

$$\mathbb{E}\left[\frac{1}{d_k^2}\right] = \frac{1}{RR_{min}}. \tag{17}$$

For proof of (17), see Appendix D. Therefore, (16) can be re-expressed as

$$C \leq K\log_2\left(1 + \frac{\rho M \eta}{RR_{min}}\right). \tag{18}$$

C. Low SNR Regime

For the low SNR regime, we have the following approximation: $\log_2(1+x) \approx x\log_2(e)$, when $x \ll 1$, then (6) can be expressed as

$$\begin{aligned} C &\approx K\mathbb{E}\left[\frac{\rho M \eta}{d_k^2}\log_2\left(e\right)\right] \\ &= K\rho M \eta \log_2\left(e\right)\mathbb{E}\left[\frac{1}{d_k^2}\right] \\ &= \frac{K\rho M \eta \log_2\left(e\right)}{RR_{min}}. \end{aligned} \tag{19}$$

In (19), we see that the sum-capacity linearly increases with the average SNR, ρ, and/or with the number of antennas, M.

Preprints (www.preprints.org) | NOT PEER-REVIEWED | Posted: 3 November 2019 doi:10.20944/preprints201911.0021.v1

$$C = \frac{K}{(R - R_{min})} \frac{2\sqrt{\rho M \eta}\left(\tan^{-1}\left(\sqrt{\frac{\rho M \eta}{R_{min}^2}}\right) - \tan^{-1}\left(\sqrt{\frac{\rho M \eta}{R^2}}\right)\right) + R\log\left(\frac{\rho M \eta}{R^2} + 1\right) - R_{min}\log\left(\frac{\rho M \eta}{R_{min}^2} + 1\right)}{\log(2)}. \quad (9)$$

$$C \approx \frac{K}{(R - R_{min})} \frac{\log(\rho M \eta)(R - R_{min}) + 2\left[R - R_{min} - R\log(R) + R_{min}\log(R_{min})\right]}{\log(2)}. \quad (10)$$

D. High SNR Regime

For the high SNR regime, we have the following approximation: $\log_2(1+x) \approx \log_2(x)$, when $x \gg 1$, then (6) can be expressed as

$$\begin{aligned} C &\approx K\mathbb{E}\left[\log_2\left(\frac{\rho M \eta}{d_k^2}\right)\right] \\ &= \frac{K}{2(R - R_{min})}\int_{1/R^2}^{1/R_{min}^2} \log_2(\rho M \eta z)\frac{1}{z\sqrt{z}}dz, \end{aligned} \quad (20)$$

where $z = \frac{1}{d_k^2}$. Solving (20) with an integral solver [23], we find an exact closed-form expression for the capacity when the channel offers favorable propagation in the high SNR regime. The exact closed-form expression for the approximated sum-capacity in (20) is given by (10).

In (10), differently from (19), we see that the sum-capacity logarithmically increases with the average SNR, ρ, and/or with the number of antennas, M. Therefore, in the high SNR regime, an increase in the transmit power and/or in the number of antennas, M, is much less impressive than in the low SNR regime case.

E. Instantaneous Sum-Capacity PDF In High SNR Regime and Favorable Propagation Condition

The instantaneous sum-capacity in high SNR regime and favorable propagation condition is given by

$$\begin{aligned} C_{\text{inst.}} &= \sum_{k=1}^{K}\log_2\left(1 + \frac{\rho M \eta}{d_k^2}\right) \\ &\overset{\frac{\rho M \eta}{d_k^2} \gg 1}{\approx} \sum_{k=1}^{K}\log_2\left(\frac{\rho M \eta}{d_k^2}\right), \end{aligned} \quad (21)$$

which is a random variable that depends on the distance of the kth device to the BS, denoted by d_k. As we will show in section V, the PDF of this random variable can be approximated by the Gamma PDF with parameters κ and θ given by (24) and (25), respectively, where $a = \log(\rho M \eta)$, $b = \log\left(\frac{\rho M \eta}{R_{\text{min}}^2}\right)$, $c = \log\left(\frac{\rho M \eta}{R^2}\right)$, $d = \log\left(\frac{1}{R_{\text{min}}^2}\right)$, and $e = \log\left(\frac{1}{R^2}\right)$. Based on knowledge of the approximated PDF, it is possible to use the Gamma's CDF as a way to analyse the outage probability, C_{out}, in high SNR regimes. Results comparing the PDF and CDF of the actual random variable and those of a Gamma random variable are presented and discussed in section V. Outage probability is the probability that a certain sum-capacity cannot be reached and is defined as

$$\begin{aligned} P_{\text{out}} &= \Pr\{C_{\text{inst.}} < C_{\text{out}}\} & (22) \\ &\overset{M \to \infty}{\approx} \frac{1}{\Gamma(\kappa)}\gamma\left(\kappa, \frac{C_{\text{out}}}{\theta}\right), & (23) \end{aligned}$$

where $\Gamma(.)$ is the gamma function, $\gamma(.,.)$ is the incomplete gamma function, and κ and θ are given by (24) and (25), respectively.

IV. Average Distance from Favorable Propagation

The favorable propagation is a important metric which is defined as mutual orthogonality among the vector-valued channels to the terminals [25]. The measure is one of the key properties of the radio channel that is exploited in Massive MIMO. From [25], we can further characterize favorable propagation as

$$\Delta_C = \frac{K\mathbb{E}\left[\log_2(1 + \rho M \beta_k)\right] - \mathbb{E}\left[\log_2|I_K + \rho \mathbf{G}^H\mathbf{G}|\right]}{\mathbb{E}\left[\log_2|I_K + \rho \mathbf{G}^H\mathbf{G}|\right]}. \quad (26)$$

As can be seen from (26), when $\Delta_C = 0$, the channel offers favorable propagation. The measure defined in (26) is an extension of the one presented in [1] for the ergodic capacity case assumed in this work.

V. Simulation Results and Discussion

Figure 2 has the following simulation setup parameters $K = 10$, $\rho = 50$ [dB], $R = 100$ [m], $R_{min} = 10$ [m], and $\lambda = 0.375$ [m], which is equivalent to a carrier frequency of 800 MHz. As can be seen, the simulated capacity is within the lower and upper bound ranges as expected. It is also possible to see that the simulated and analytical capacities in favorable propagation match each other, showing that the derived analytical closed-form is tight for the favorable propagation case. Moreover, the simulated capacity asymptotically approaches the capacity in favorable propagation as the number of antennas, M, grows, proving that favorable propagation is asymptotically achieved as M grows. It is also important to highlight that the analytical capacity in favorable propagation, given by (9), provides a good approximation for the capacity. For example, for $M = 100$ the simulated capacity is equal to 23.59 bits/s/Hz and the analytical capacity in favorable propagation is equal to 24.44 bits/s/Hz.

Figure 2 also presents on the right x-axis the average distance from favorable propagation as defined in (26). As can be noticed, the average distance asymptotically decreases as the number of antennas grows, starting at 0.14 for $M = 10$ and decreasing to 0.0049 for $M = 1000$. This result is

Preprints (www.preprints.org) | NOT PEER-REVIEWED | Posted: 3 November 2019 doi:10.20944/preprints201911.0021.v1

$$\kappa = \frac{\frac{K}{(R-R_{\min})}\left(\frac{b+2}{R} - \frac{c+2}{R_{\min}}\right)^2}{\frac{1}{RR_{\min}}\left(\frac{2e(a+2)+e^2+a(a+4)+8}{R_{\min}} - \frac{2d(a+2)+d^2+a(a+4)+8}{R}\right) - \frac{1}{(R-R_{\min})}\left(\frac{b+2}{R} - \frac{c+2}{R_{\min}}\right)^2}. \quad (24)$$

$$\theta = \frac{\frac{RR_{\min}}{(R-R_{\min})}\left(\frac{b+2}{R} - \frac{c+2}{R_{\min}}\right)^2 - \frac{2e(a+2)+e^2+a(a+4)+8}{R_{\min}} + \frac{2d(a+2)+d^2+a(a+4)+8}{R}}{\log(2)\left(\frac{b+2}{R} - \frac{c+2}{R_{\min}}\right)}. \quad (25)$$

another indication that favorable propagation is asymptotically achieved as M grows.

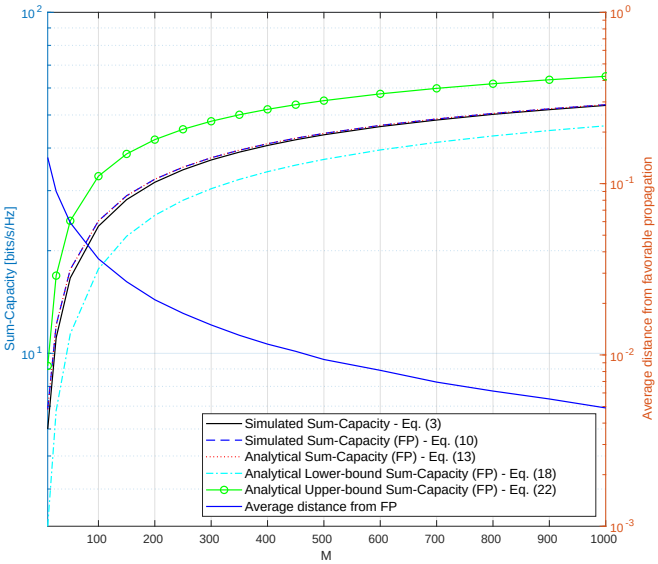

Figure 2. Simulation considering $K = 10$, $\rho = 50$ [dB], $R = 100$ [m], $R_{min} = 10$ [m], and $\lambda = 0.375$ [m].

Figure 3 compares the sum-capacity over the variation of the average SNR, ρ, for the same simulation parameters used for the results in Figure 2 and M constant equal to 300 antennas. As expected, the sum-capacity, simulated and analytical, stay within the lower and upper capacity bounds. For low SNR values the sum-capacity is closer to the upper bound and as the SNR increases, we see that both lower and upper bounds converge to the sum-capacity.

In Figure 4 we present the results of the sum-capacity for low and high SNR regimes in favorable propagation condition versus the average signal-to-interference ratio, ρ, with M constant and equal to 300 antennas. As can be seen, (19) and (10) represent the sum-capacity fairly well for the low and high SNR regimes, respectively. In the upper part of the figure, we show the sum-capacity for the low SNR regime and it is possible to see that the approximated expression given by (19) closely follows the sum-capacity until around 30 [dB]. In the lower part of the figure, we show the sum-capacity for the high SNR regime and we also see that the approximated expression given by (10) closely follows the sum-capacity for SNR values greater than 40 [dB]. The figure also shows that the sum-capacity grows linearly and logarithmically with the average SNR for the low and high SNR regimes, respectively,

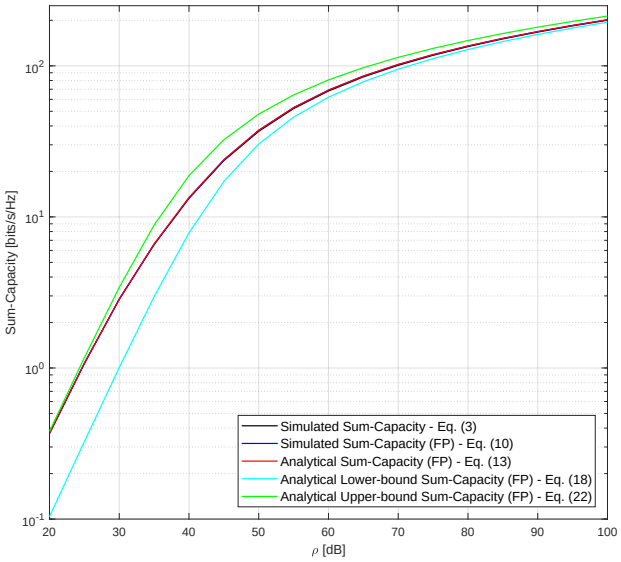

Figure 3. Simulated and analytical sum-capacity considering $M = 300$.

confirming what was discussed in subsections III-C and III-D

Figure 5 shows how the spectral efficiency behaves as $\rho = P/M^{\alpha}$, where $\alpha = 1/2, 1$ and $3/2$, respectively. The following simulation setup parameters were used: $K = 10$, $P = 50$ [dB], $R = 100$ [m], $R_{min} = 10$ [m], and $\lambda = 0.375$ [m]. As expected and stated in Remark 1, when $\alpha = 1$ and M increases, the capacity becomes constant no matter the number of antennas. However, when $\alpha = 1/2$ the capacity grows logarithmically fast with M when $M \to \infty$ and tends to zero when $\alpha = 3/2$ and $M \to \infty$. These results attest that the transmit power of each device can be reduced proportionally to M.

In Figure 6 we show the required transmit power per device that is needed to achieve fixed capacities of 1 and 2 bits/s/Hz respectively. As expected and predicted by Remark 1, the transmit power can be reduced by approximately 3 [dB] by doubling the number of antennas, M, for both cases, $i.e.$, 1 and 2 bits/s/Hz.

Figure 7 shows the comparison between the normalized histogram of the random variable Z, where Z is defined in Lemma 1, and the Gamma PDF for number of devices equal to $K = 10$, 20, and 50 respectively. These results were also obtained with the following simulation setup parameters $K = 10$, $\rho = 50$ [dB], $R = 100$ [m], $R_{min} = 10$ [m], and $\lambda = 0.375$ [m]. The histogram, showed in blue, is the

Preprints (www.preprints.org) | NOT PEER-REVIEWED | Posted: 3 November 2019 doi:10.20944/preprints201911.0021.v1

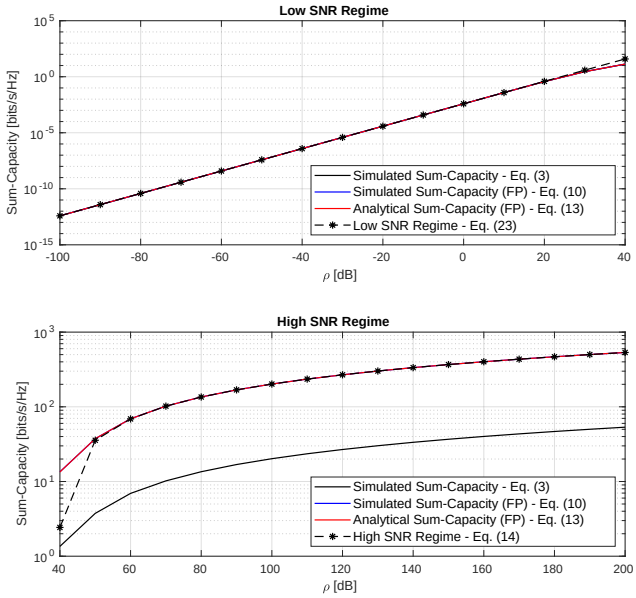

Figure 4. Sum-capacity for low and high SNR regimes versus average signal-to-interference ratio, ρ.

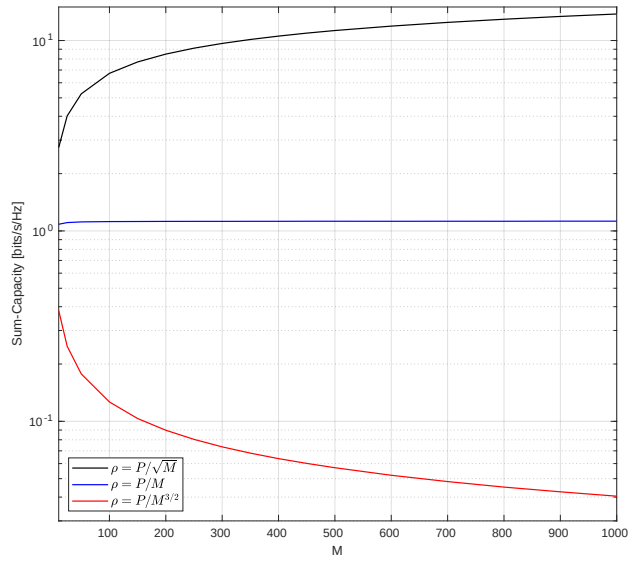

Figure 5. Demonstration of the power scaling law for different α values.

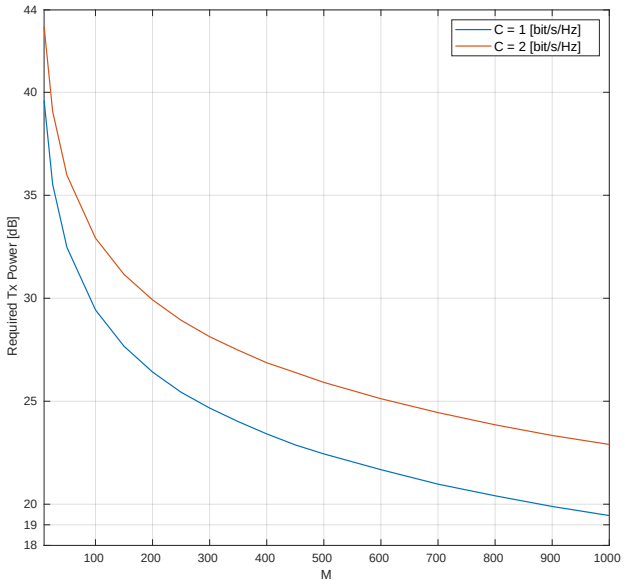

Figure 6. Required transmit power to achieve 1 and 2 bits/s/Hz as a function of the number of antennas.

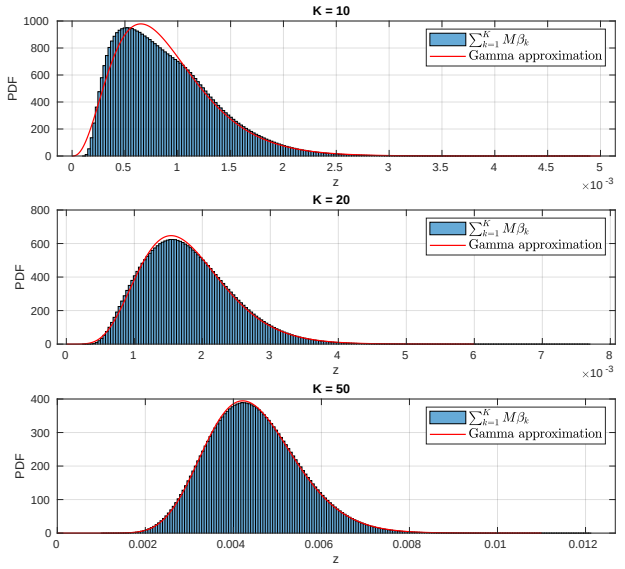

Figure 7. Gamma PDF for number of devices equal to $K = 10$, 20, and 50 respectively.

histogram of the random variable $Z = \sum_{k=1}^{K} M\beta_k$. As can be seen, the histogram approaches the Gamma PDF as the number of devices increases.

Figure 8 comparison of the instantaneous sum-capacity in high SNR regime and favorable propagation condition and its approximation with the Gamma PDF. This comparison was obtained with the following parameters $K = 10$, $\rho = 60$ [dB], $R = 100$ [m], $R_{min} = 10$ [m], and $\lambda = 0.375$ [m]. As can be seen, for high SNR, the Gamma PDF fits the PDF of the instantaneous sum-capacity random variable as the number of antennas grows.

Figure 9 presents the comparison between the approximated and simulated outage probabilities in the high SNR regime and favorable propagation condition. The simulation parameters are the same used for generating the results in Figure 8. As can be also seen, for high SNR, the Gamma CDF fits the simulated outage probability of the instantaneous sum-capacity random variable as the number of antennas grows.

VI. Conclusions

In this work, we investigated ways to find capacity limits concerning the number of users, number of base station antennas, and SNR. By assuming a dominant LOS environment in a massive MIMO scenario with favorable propagation, it was possible to derive analytical expressions for the channel capacity. Convenient simplifications on expressions were possible working at low and high SNR regimes. Furthermore, in the case of high SNR, it is demonstrated that the Gamma PDF can approximate the PDF of the instantaneous channel sum-capacity as the number of antennas grows. A second important

Preprints (www.preprints.org) | NOT PEER-REVIEWED | Posted: 3 November 2019 doi:10.20944/preprints201911.0021.v1

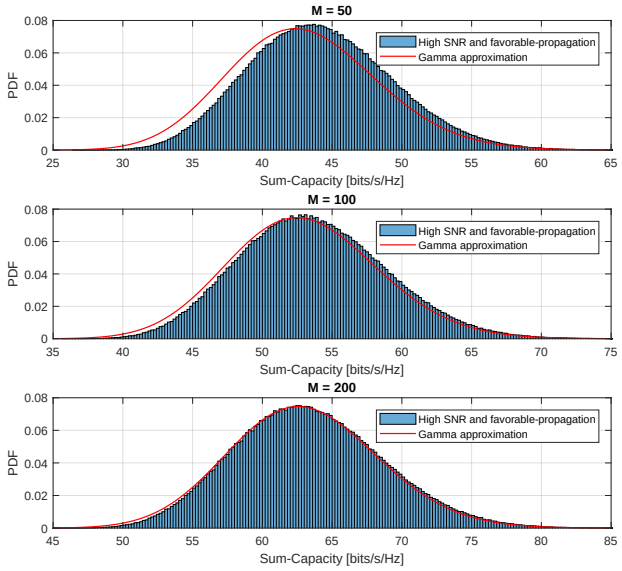

Figure 8. Comparison of the approximated PDF for the instantaneous sum-capacity in high SNR regime and favorable propagation condition.

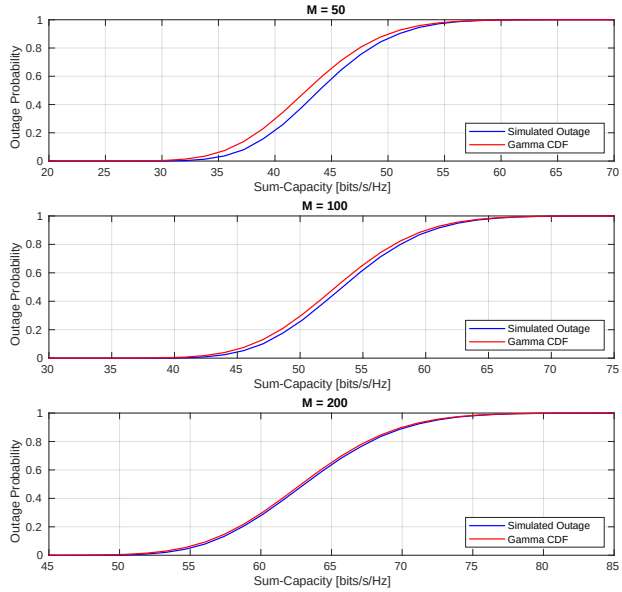

Figure 9. Comparison between the approximated and simulated outage probabilities in high SNR regime and favorable propagation condition.

demonstration is that a Gamma PDF can also approximate the PDF of the summation of the channel's singular values as the number of devices increases. Finally, the utility of such a framework is useful for LPWAN's as we show that the transmit power of each device can be made inversely proportional to the number of BS antennas.

Appendix A
Derivation of $\|\mathbf{g}_k\|^2 = M\beta_k$

From (1), and using the very definition of the product of two matrices [26], we can write each element $g_{i,j}$ as

$$g_{i,j} = \sum_{l=1}^{K} h_{i,l}\sqrt{q_{l,j}} \tag{27}$$

since $\mathbf{Q}$ is a diagonal matrix,

$$g_{i,l} = h_{i,l}\sqrt{q_{l,l}}. \tag{28}$$

Therefore

$$\|\mathbf{g}_k\|^2 = \sum_{i=1}^{M} \left|h_{i,k}\sqrt{q_{k,k}}\right|^2 = \sum_{i=1}^{M} |h_{i,k}|^2 \left|\sqrt{q_{k,k}}\right|^2, \tag{29}$$

where $|h_{i,k}|^2 = 1$ and $\left|\sqrt{q_{k,k}}\right|^2 = \beta_k$, therefore

$$\|\mathbf{g}_k\|^2 = \sum_{i=1}^{M} \beta_k = M\beta_k. \tag{30}$$

Appendix B
Derivation of the PDF of the distance random variable

Given that the PDF of Y is defined as

$$f_Y(y) = \frac{1}{R - R_{min}}, \quad R_{min} \leq y \leq R, \tag{31}$$

and the strictly monotonic differentiable function $Z = g(Y) = 1/Y^2$, then the PDF of Z is given by

$$f_Z(z) = \frac{f_Y(g^{-1}(Z))}{|g'(Y)|}, \tag{32}$$

where $g'(Y) = -2/Y^3$ and $g^{-1}(Z) = 1/\sqrt{Z}$. Therefore,

$$\begin{aligned} f_Z(z) &= \frac{f_Y(g^{-1}(Z))}{|g'(Y)|} = \frac{\frac{1}{R-R_{min}}}{|\frac{-2}{y^3}|} \\ &= \frac{1}{2(R - R_{min})z\sqrt{z}}, \end{aligned} \tag{33}$$

where in the last equality we used the fact that $y = 1/\sqrt{z}$.

Appendix C
Gamma PDF and users

Lemma 1: Let $\beta_k = \eta/d_k^2$, where d_k is uniformly distributed with PDF given by $1/(R - R_{min})$, therefore, the PDF of $Z = \sum_{k=1}^{K} M\beta_k$ can be approximated by the Gamma distribution with parameters $\kappa = \frac{3KRR_{min}(R-R_{min})}{(R^3-R_{min}^3)-3RR_{min}(R-R_{min})}$ and $\theta = \eta M \frac{(R^3-R_{min}^3)-3RR_{min}(R-R_{min})}{3R^2R_{min}^2(R-R_{min})}$.

Appendix D
Calculation of the expected values of d_k^2 and $1/d_k^2$

A. Calculation of $\mathbb{E}\left[d_k^2\right]$

$$\mathbb{E}\left[d_k^2\right] = \int_{R_{\min}}^{R} r^2 f_d(r) dr = \int_{R_{\min}}^{R} \frac{r^2}{R - R_{\min}} dr = \frac{R^3 - R_{min}^3}{3(R - R_{min})}. \tag{34}$$

B. Calculation of $\mathbb{E}\left[\frac{1}{d_k^2}\right]$

$$\mathbb{E}\left[\frac{1}{d_k^2}\right] = \int_{R_{\min}}^{R} \frac{1}{r^2} f_d(r) dr = \int_{R_{\min}}^{R} \frac{1}{r^2(R - R_{\min})} dr = \frac{1}{RR_{min}}. \tag{35}$$

ACKNOWLEDGMENT

This work was funded by the European Union's Horizon 2020 research and innovation programme under grant agreement No. 732174 (ORCA project). Additionally, this work was partially supported by R&D ANEEL - PROJECT COPEL 2866-0366/2013. This work was partially funded by EMBRAPII - Empresa Brasileira de Pesquisa e Inovacao Industrial. E. R. Lima was supported in part by CNPq under Grant 313239/2017-7. G. Fraidenraich was supported in part by CNPq under Grant 304946/2016-8.

REFERENCES

[1] T. L. Marzetta, *Fundamentals of massive MIMO*. Cambridge University Press, 2016.

[2] E. Björnson, L. Sanguinetti, H. Wymeersch, J. Hoydis, and T. L. Marzetta, "Massive mimo is a reality—what is next?: Five promising research directions for antenna arrays," *Digital Signal Processing*, vol. 94, pp. 3 – 20, 2019.

[3] K. Haneda, J. Zhang, L. Tan, G. Liu, Y. Zheng, H. Asplund, J. Li, Y. Wang, D. Steer, C. Li, *et al.*, "5G 3GPP-like channel models for outdoor urban microcellular and macrocellular environments," in *2016 IEEE 83rd Vehicular Technology Conference (VTC Spring)*, pp. 1–7, IEEE, 2016.

[4] Z. Pi, J. Choi, and R. Heath, "Millimeter-wave gigabit broadband evolution toward 5G: Fixed access and backhaul," *IEEE Communications Magazine*, vol. 54, no. 4, pp. 138–144, 2016.

[5] E. Bjornson, L. Van der Perre, S. Buzzi, and E. G. Larsson, "Massive MIMO in sub-6 GHz and mmWave: Physical, practical, and use-case differences," *IEEE Wireless Communications*, vol. 26, no. 2, pp. 100–108, 2019.

[6] H. Yang and T. L. Marzetta, "Energy Efficiency of Massive MIMO: Cell-Free vs. Cellular," in *2018 IEEE 87th Vehicular Technology Conference (VTC Spring)*, pp. 1–5, IEEE, 2018.

[7] S. A. Hassan, M. S. Omar, M. A. Imran, J. Qadir, and D. Jayako, "Universal access in 5G networks, potential challenges and opportunities for urban and rural environments," *5G Networks: Fundamental Requirements, Enabling Technologies, and Operations Management*, 2017.

[8] W. K. Pan and R. E. Bilsborrow, "The use of a multilevel statistical model to analyze factors influencing land use: a study of the ecuadorian amazon," *Global and Planetary Change*, vol. 47, no. 2-4, pp. 232–252, 2005.

[9] L. Gonsioroski, M. C. de Almeida, P. Castellanos, D. Okamoto, J. Arnez, R. Souza, and L. da Silva Mello, "Preliminary results of channel characterization at 700mhz band in urban and rural regions," in *2014 International Telecommunications Symposium (ITS)*, pp. 1–5, IEEE, 2014.

[10] J. Van Rees, "Measurements of the wide-band radio channel characteristics for rural, residential, and suburban areas," *IEEE Transactions on Vehicular Technology*, vol. 36, no. 1, pp. 2–6, 1987.

[11] P. Chandhar, D. Danev, and E. G. Larsson, "Massive MIMO as enabler for communications with drone swarms," in *2016 International Conference on Unmanned Aircraft Systems (ICUAS)*, pp. 347–354, IEEE, 2016.

[12] E. Becirovic, E. Björnson, and E. G. Larsson, "How much will tiny iot nodes profit from massive base station arrays?," in *2018 26th European Signal Processing Conference (EUSIPCO)*, pp. 832–836, IEEE, 2018.

[13] P. Chandhar and E. G. Larsson, "Massive mimo for connectivity with drones: Case studies and future directions," *IEEE Access*, vol. 7, pp. 94676–94691, 2019.

[14] P. Chandhar, D. Danev, and E. G. Larsson, "On the zero-forcing receiver performance for massive MIMO drone communications," in *2018 IEEE 19th International Workshop on Signal Processing Advances in Wireless Communications (SPAWC)*, pp. 1–5, IEEE, 2018.

[15] A. Garcia-Rodriguez, G. Geraci, D. López-Pérez, L. G. Giordano, M. Ding, and E. Björnson, "The Essential Guide to Realizing 5G-Connected UAVs with Massive MIMO," *arXiv preprint arXiv:1805.05654*, 2018.

[16] P. Chandhar, D. Danev, and E. G. Larsson, "On ergodic rates and optimal array geometry in line-of-sight massive MIMO," in *2016 IEEE 17th International Workshop on Signal Processing Advances in Wireless Communications (SPAWC)*, pp. 1–6, IEEE, 2016.

[17] C. A. Balanis, *Antenna Theory: Analysis and Design*. Wiley Interscience, 2005.

[18] D. Tse and P. Viswanath, *Fundamentals of Wireless Communication*. New York, NY, USA: Cambridge University Press, 2005.

[19] H. Q. Ngo, E. G. Larsson, and T. L. Marzetta, "Energy and Spectral Efficiency of Very Large Multiuser MIMO Systems," *IEEE Transactions on Communications*, vol. 61, pp. 1436–1449, April 2013.

[20] A. L. Giuseppa Alfano and S. Verdu, "Mutual Information and Eigenvalue Distribution of MIMO Ricean Channels," in *International Symposium on Information Theory and its Applications (ISITA2004)*, 2004.

[21] Z. Chen and E. Björnson, "Channel hardening and favorable propagation in cell-free massive MIMO with stochastic geometry," *IEEE Transactions on Communications*, vol. 66, no. 11, pp. 5205–5219, 2018.

[22] J. H. Emil Bjornson and L. Sanguinetti, *Massive MIMO Networks: Spectral, Energy, and Hardware Efficiency*. Now Publishers, 2017.

[23] Wolfram Research, "Mathematica," 2018.

[24] T. M. Cover and J. A. Thomas, *Elements of Information Theory (Wiley Series in Telecommunications and Signal Processing)*. New York, NY, USA: Wiley-Interscience, 2006.

[25] H. Q. Ngo, E. G. Larsson, and T. L. Marzetta, "Aspects of favorable propagation in massive MIMO," in *2014 22nd European Signal Processing Conference (EUSIPCO)*, pp. 76–80, IEEE, 2014.

[26] R. A. Horn and C. R. Johnson, *Matrix Analysis*. New York, NY, USA: Cambridge University Press, 2nd ed., 2012.